Supporting Information

‘End-to-End’ stacking of small dsRNA

Erlenbach, Nicole[1], Grünewald, Christian[2], Krstic, Bisera[1], Heckel, Alexander[2] and Prisner, Thomas F.[1,*]

[1] Institute of Physical and Theoretical Chemistry and Center of Biomolecular Magnetic Resonance, Goethe University, D-60438 Frankfurt am Main, Germany

[2] Institute of Organic Chemistry and Chemical Biology, Goethe-University Frankfurt, D-60438 Frankfurt am Main, Germany

4-pulse PELDOR background correction

Original 4-pulse PELDOR time trace and the assumed non-specific background function for the time trace of Figure 2e in the manuscript is depictured in Figure S1.

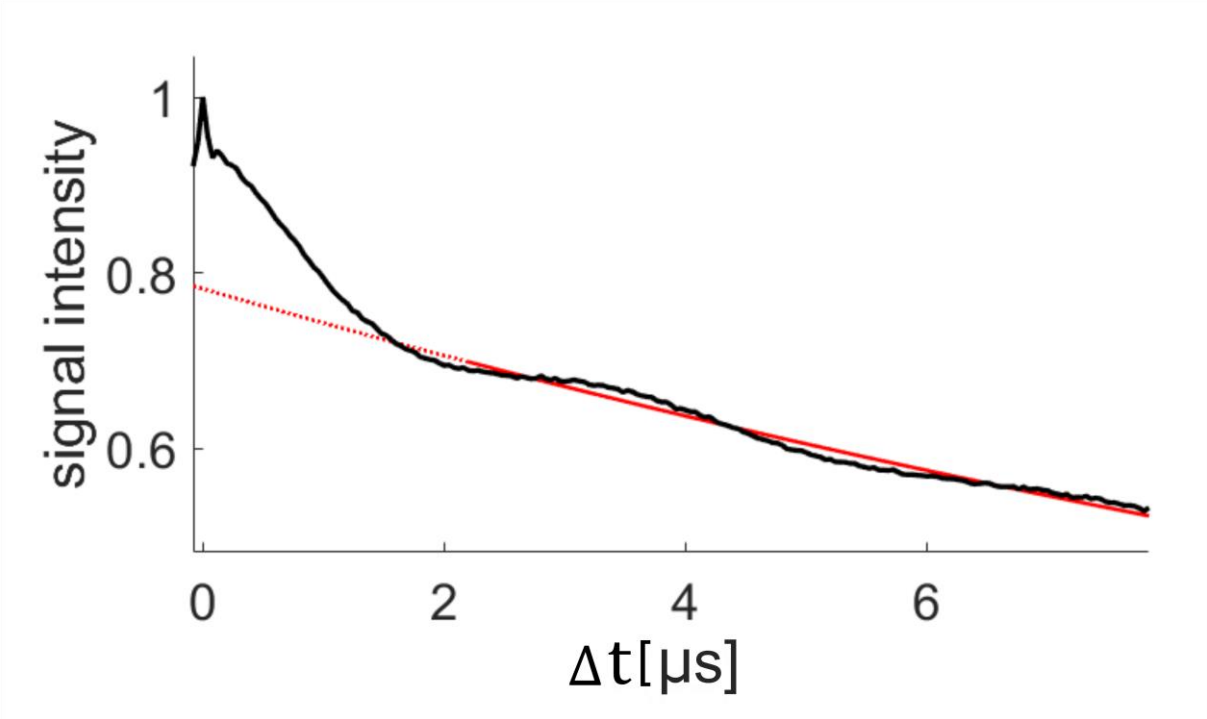

Figure S1 Background correction for the 4-Pulse PELDOR time traces of singly labelled dsRNA without overhang

7-pulse CP-PELDOR background correction

The 7-pulse CP-PELDOR experiments (Figure 2g) exhibit three inversion pulses for the coupled spin. Despite the fact that adiabatic sech/tanh inversion pulses are applied, the inversion efficiency is not perfect. This leads to unwanted signal contributions arising from spins where two or one of the inversion pulses only inverts the coupled spin. With our published procedure (Spindler et al. 2015) an undisturbed time trace (Figure 2h) can be derived. All correction steps to obtain the final dipolar time trace shown in Figure 2h are depictured in Figure S2.

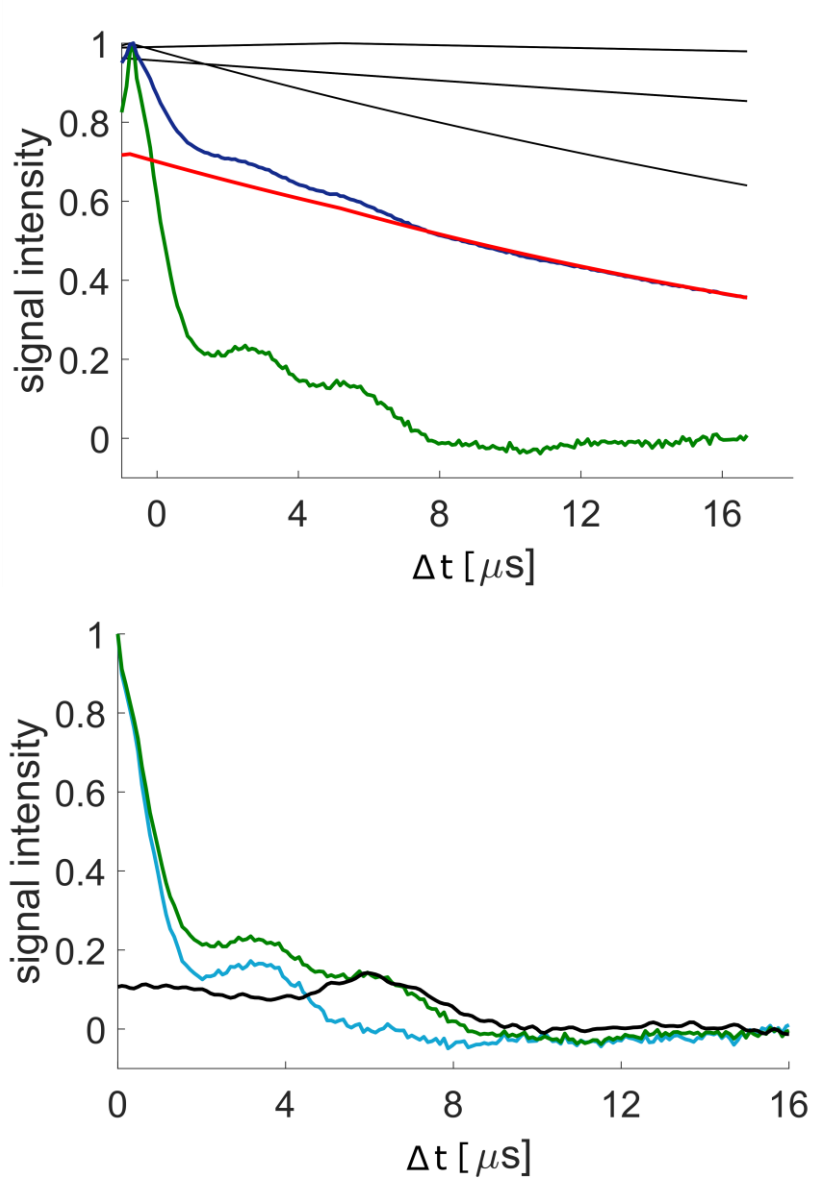

Figure S2 7-pulse CP-PELDOR data of singly labelled dsRNA without overhang. Top figure: The experimental raw time trace is shown in blue. In black are shown the decay functions for the different possible dipolar pathways. The product of all of them is shown in red. The background corrected dipolar signals after subtraction of the unmodulated part and renormalization is shown in green. Bottom figure: Background corrected PELDOR time trace in green and the artefact corrected time trace (light blue). The sum of all artefacts is shown in black.

Determination of modulation depths parameter Δ

The modulation depths reported in Figure 3 and 4 of the main text were extracted from the following raw PELDOR time traces (Figure S3).

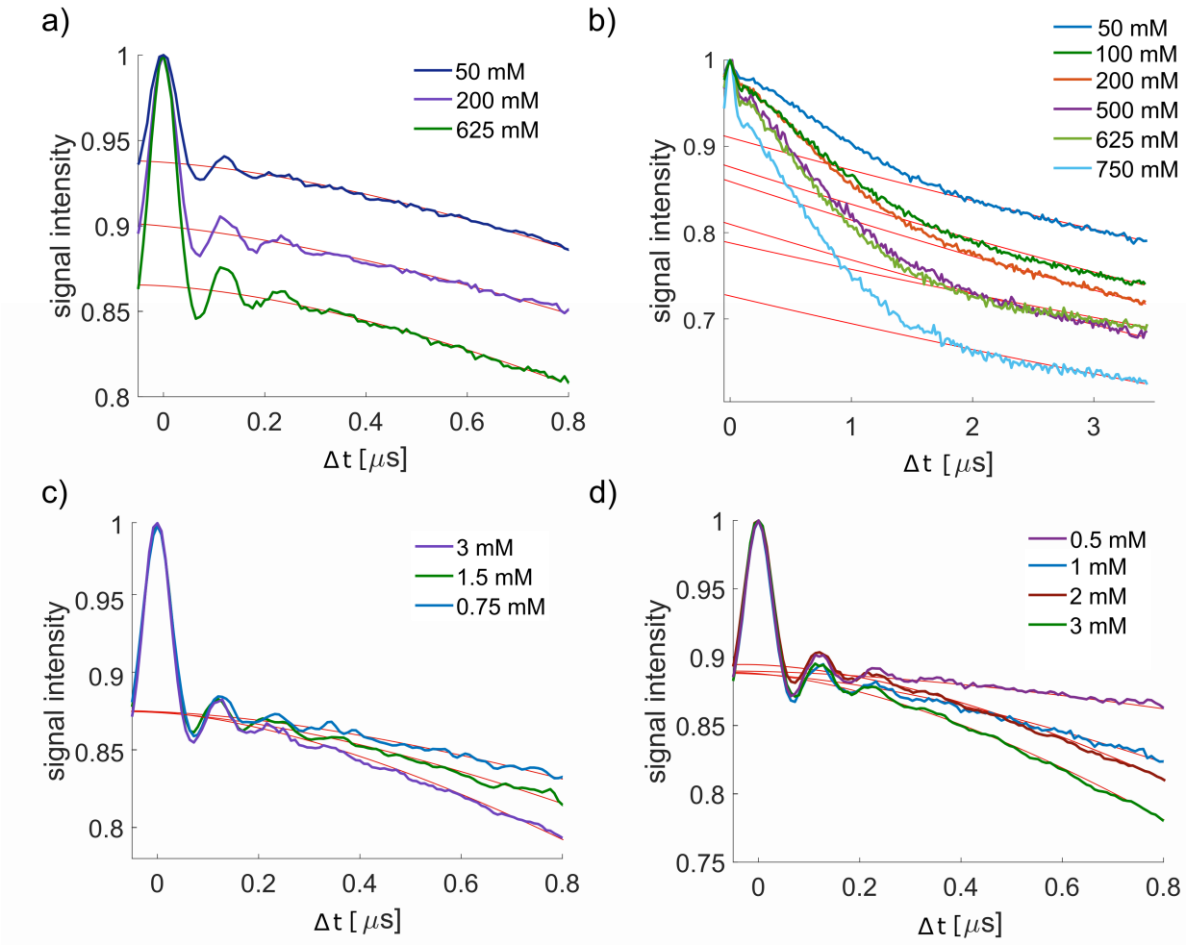

Figure S3 Raw 4-pulse-PELDOR traces of singly labelled dsRNA. a) Time traces of dsRNA samples with one nucleotide overhang for three different monovalent NaCl salt concentration as depicted in the figure legend. b) Time traces of dsRNA samples without any overhang for six different salt concentration as depicted in the figure legend. c) and d) Time traces of dsRNA samples with one nucleotide overhang for different RNA concentrations as depicted in the figure legends. c) Experiments for a salt concentration of 500 mM and d) for a salt concentration of 200 mM.

For short times Δt < 0.8 μs ,the background deviated slightly from a straight exponential. Therefore, for the singly labelled dsRNA with one nucleotide overhang a higher dimensional (D=4) background was used. This higher dimensional background might be due to a very small remnant stacking probability between the protected ends or to an excluded volume effect. As demonstrated in Figure S4, such uncertainties in the determination of the background function does only very weakly influence the determination of the modulation depth parameter Δ. This uncertainty was taken into account and reflects the error bars of the stacking probabilities *p* shown in all figures.

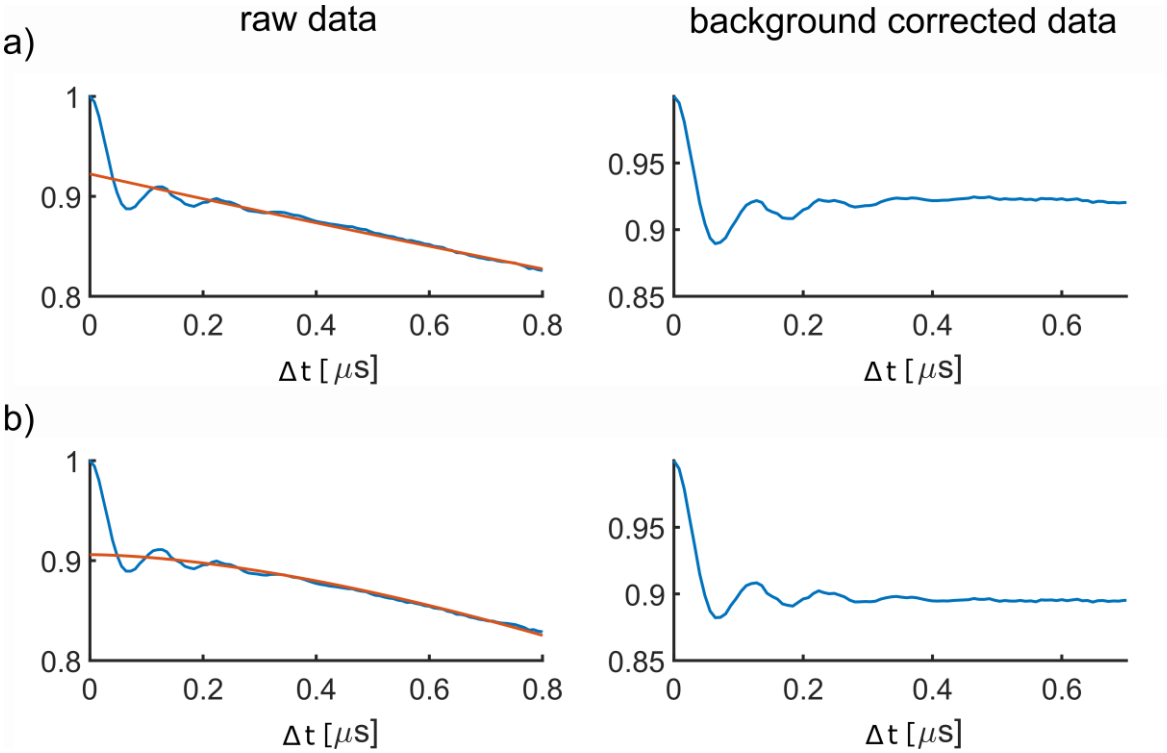

Figure S4 Background correction for the 4-pulse PELDOR time traces of singly labelled dsRNA with one overhang. On the left side, the original experimental data are shown in blue and the background in red. On the right side, the background corrected form factors are depictured. Background correction was done with DeerAnalysis in a) with a three dimensional background and in b) with a four dimensional background. As can be seen the chosen background dimensionality does only slightly affect the value for the modulation depth (<5%).

Detection of the excitation efficiency λ

To detect the excitation efficiency λ a nitroxide biradical (Schöps et al. 2015, structure depicted in Figure S5) was measured with the same pulse parameter than the dsRNA samples. As for the model compound all spins are quantitatively dipolar coupled, the modulations depth only depends on the excitation frequency. An excitation efficiency of 0.36±0.05 was determined from three independent measurements (Figure S5).

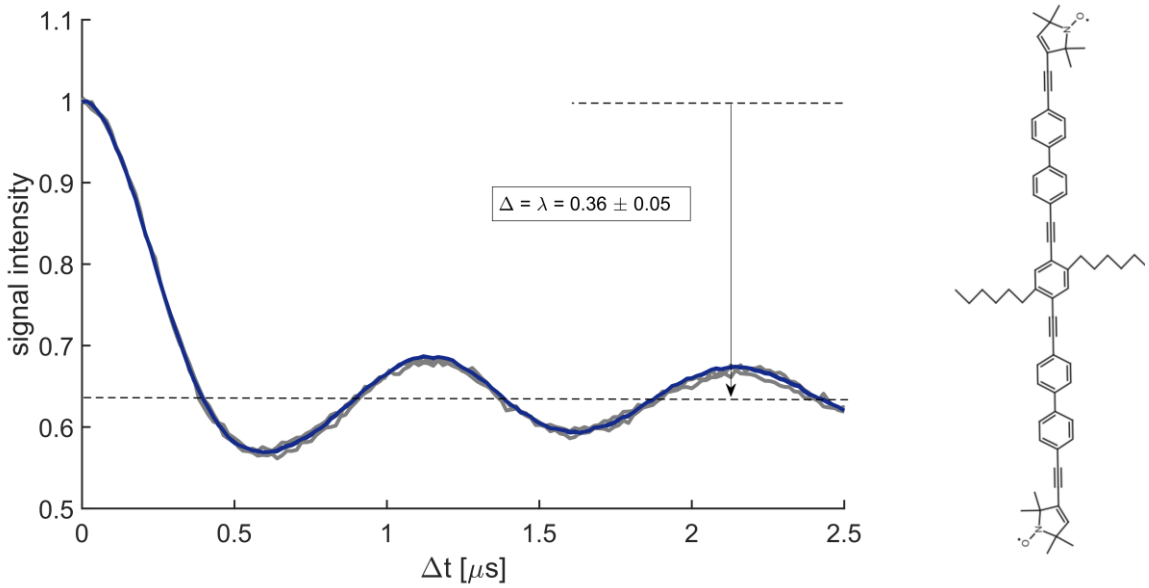

Figure S5 Three background corrected 4-pulse-PELDOR time traces (two shown in gray and one in blue) measured with the binitroxide model compound shown on the right.

Stacking probability *p* and dissociation constant K_d for samples with different RNA concentrations

To confirm that K_d only depends on the salt-to-RNA ratio *R* and not the absolute salt concentration, we have measured two samples with an equal salt-to-RNA ratio of 2000 but with different RNA concentrations. The signal time trace for the sample with higher RNA concentration (blue PELDOR time trace, Figure S6a) has an increased modulation depth Δ and therefore a higher stacking probability *p* compared to the time trace with lower RNA concentration (black curve). Both data points for *p* fit within experimental error to equation [5], described in the manuscript for a dissociation constant K_d = 460 µM. This dissociation constant was read-off from Figure 4b for a fixed salt-to-RNA ratio of *R*=2000.

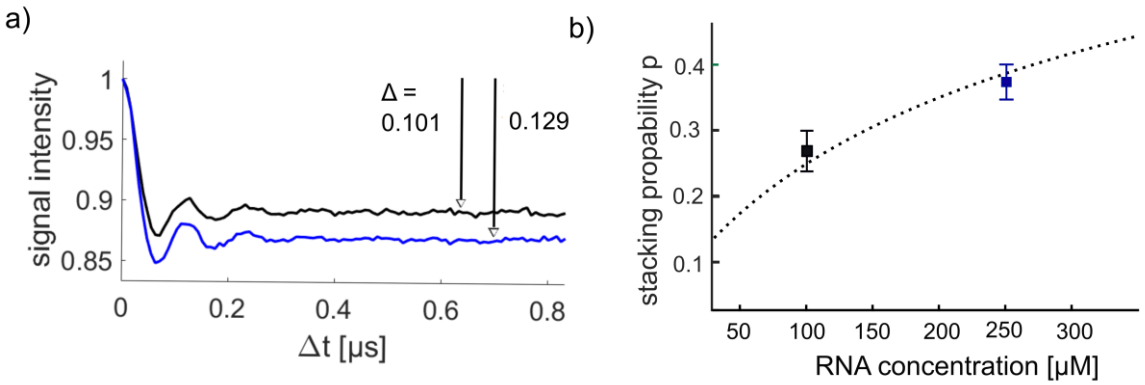

Figure S6 (a) PELDOR measurements with RNA duplexes having one overhang. Both samples are different in their RNA concentration but identical in their salt-to-RNA ratio. Black: c(RNA) =100 µM; c(NaCl)= 200 mM. Blue: (c(RNA) =250; c(NaCl)=500 mM (b) Stacking probability of dsRNA in relation to the RNA concentration. The dotted line indicate the expected behaviour following equation [5] from the main text with a constant K_d of 460µM (corresponding to a salt-to-RNA ratio of 2000, see Figure 4 main text).

Moreover it can be shown that also all the measurements with varying RNA concentrations (shown in the main text in Figure 5a) fall onto the curve $K_d(R)$ extracted from the measurements with varying salt concentration and a constant RNA concentration (Figure 4b main text). The results are shown in Figure S7.

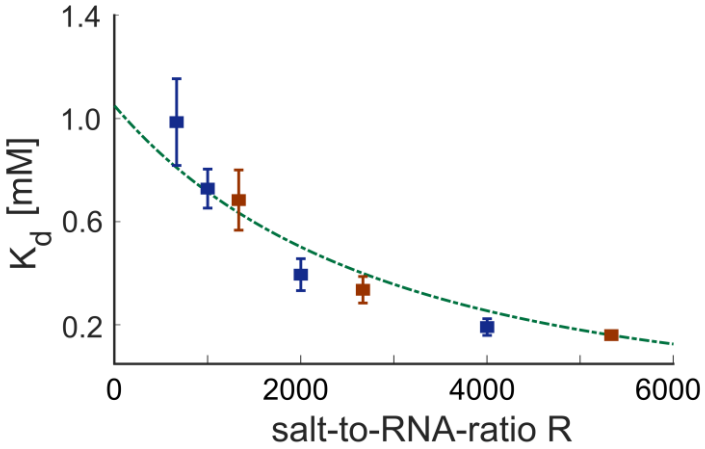

Figure S7 Dissociation constant K_d derived from experiments with different RNA concentrations and two constant salt concentration (200 mM NaCl (blue) and 500 mM NaCl (orange)). The dotted line is the K_d dependency on *R* extracted from measurements with a constant RNA concentration and different salt concentrations (Figure 4b of the main text).

Calculation of stacking probability for samples without overhang

For samples with one overhang, only dimerization of the dsRNAs is possible. However, dsRNAs without any overhang are able to form higher oligomers. As stated in the main text the modulation depth *Δ* depends on the excitation efficiency *λ* of the nitroxide spin label and the number of coupled spins *n*. If higher oligomers occur, more than two spin labels are coupled to each other. For *n* spins coupled, the modulations depth can be calculated to (Bode et al. 2005)

$$\Delta = 1 - (1 - \lambda)^{n-1} \qquad [S1]$$

with λ being the excitation efficiency defined before.

The probability for a specific oligomeric state *P(n)* depend on the stacking probability *p* of the dsRNA duplex and is given by:

$$P(n) = M\, p^{n-1} \qquad [S2]$$

with *M* being the probability of the monomer. The normalization condition $\sum P(n)=1$ and the convergence of the geometric series leads to

$$P(n) = (1 - p)p^{n-1} \qquad [S3]$$

Therefore, the overall modulation depth for dsRNA molecules without overhang can be written as:

$$\Delta = (1 - p)\sum_{n=1}^{n=\infty}(1 - (1 - \lambda)^{n-1})p^{n-1} \qquad [S4]$$

Again, the infinite sum can be written as two geometric series, leading to the following solution:

$$p = \frac{\Delta}{(\Delta + \lambda - \lambda\Delta)} \qquad [S5]$$

The experimental modulation depth Δ for measurements with (blue) and without (green) overhangs are shown in Figure S8a. The resulting stacking probabilities *p* (Figure S8b) for samples with overhang can be calculated with p=Δ/λ. For the samples without overhang, the stacking probability was calculated according equation S5. As can be seen, both samples lead to the same 'end-to-end' stacking probabilities *p*.

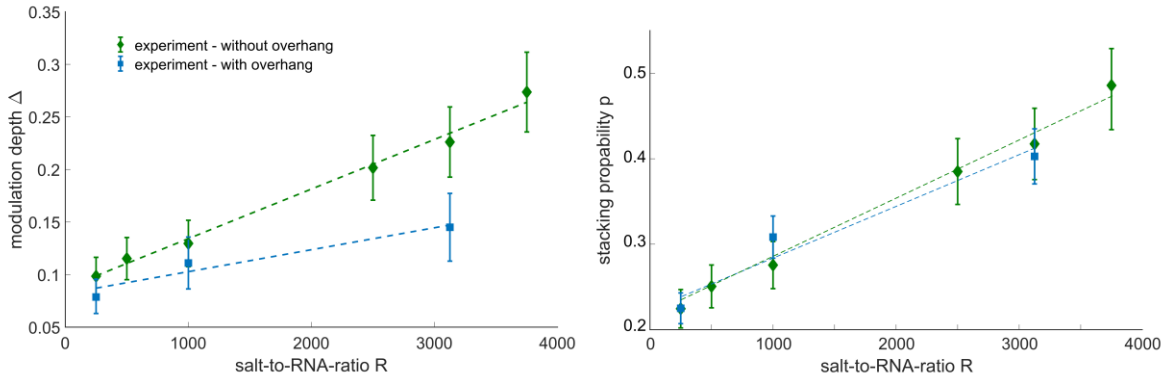

Figure S8 Dependence of the stacking probability to the salt-to-RNA ratio. Left side: Modulation depth *Δ* extracted from the PELDOR time traces. Green data points represents the measurements without overhang while the blue rectangles show the experiments from samples with one overhang. The error of the determined modulation depth was estimated to be 10 % (see above). Right side: Calculated stacking probabilities *p* for the samples with one overhang (blue) and without overhang (green). For the calculation of *p* the respective formulas were used (see above).

Literature

Bode BE, Margraf D, Plackmeyer J, Dürner G, Thomas F. Prisner A, Olav Schiemann. 2007. Counting the Monomers in Nanometer-Sized Oligomers by Pulsed Electron−Electron Double Resonance. J Am Chem Soc **129**: 6736–6745.

Schöps P, Spindler PE, Marko AM, Prisner TP. 2015. Broadband spin echoes and broadband SIFTER in EPR. J Magn Res. **250:** 55-62

Spindler PE, Waclawska I, Endeward B, Plackmeyer J, Ziegler C, Prisner TF. 2015. Carr–Purcell Pulsed Electron Double Resonance with Shaped Inversion Pulses. J Phys Chem Lett **6**: 4331–4335.